J. Biomechanics, Vol. 4, pp. 251–263. Pergamon Press, 1971. Printed in Great Britain

FLEXURE OF LAYERED CRANIAL BONE*

ROBERT P. HUBBARD†
Highway Safety Research Institute, The University of Michigan, Ann Arbor, Michigan 48105, U.S.A.

Abstract – The present study is an important step in understanding the brain case as a structure. Beams taken from the layered regions of embalmed calvaria were repeatedly tested in three-point bending at various span lengths to determine the resistance of layered cranial bone to bending and shearing deflection. These beams were also strain gaged and loaded to failure in four-point bending to study the failure response of layered cranial bone. The layered beam theory used in this study was found to provide a valid relationship between the constituent material properties and structural geometry of layered cranial bone and its flexural response.

INTRODUCTION

IN AN EFFORT to better understand traumatic head injury, mechanical and mathematical models of the human head are being developed. Essential to the development of these models is the study of the mechanical behavior of the materials and structures which constitute the human head. The brain case is a significant structure of the head in that it contains and protects the brain and is the medium through which effects of trauma often pass. The bones of the brain case are generally layered with compact inner and outer tables separated by a porous diploë layer.

As a first step in understanding the mechanical response of the brain case, the mechanical properties of its constituents have been studied (Wood, 1969; Melvin *et al.* 1969). The present study is an important step in understanding the brain case as a structure. The flexural stiffness and strength of layered cranial bone are determined experimentally using beam test techniques. Layered beam theory is used to relate the mechanical response of layered cranial bone to constituent material properties and structural geometry. Beams were chosen for study because they are the simplest structural members involving bending; they can be extensively treated theoretically, and they yield results which are significant to more complex structural geometries such as plates and shells.

SANDWICH STRUCTURES AND CRANIAL BONE

Initially developed for use in aircraft, layered panels with relatively stiff faces separated by lighter, lower stiffness cores are generally stiffer and stronger for their weight than homogeneous panels. The similarity between the layered regions of human cranial bone and man-made sandwich structures is interesting because of the efficiency of the natural structure and the prospect of applying sandwich structure technology to the study of layered cranial bone.

When a layered panel is transversely loaded, four types of deformation lead to transverse deflection: (1) membrane deformation, (2) bending deformation, (3) shear deformation, and (4) local core compression and puncture of the skull. Membrane deformation is a stretching or compressing of the layered structure in the plane of the panel and is resisted by normal stresses which are evenly distributed across a transverse section. Membrane deformation leads to resultant forces (N_{fm}) in the faces which are equal

*Received 20 January 1971.
†Postdoctoral Fellow.

in magnitude and in the same direction (Fig. 1b). Because the beam core is much less stiff than the faces, forces developed in the core due to membrane deformation are usually insignificant. Membrane stiffness of skull bone has been determined by McElhaney *et al.* (1970) by compression testing of cranial bone samples in a direction perpendicular to a radial line.

Bending deformation causes a change in the curvature of a layered panel and is resisted by a normal stress distribution which changes from tensile in one face to compressive in the other face. Bending of a layered beam leads to resultant forces in the faces (N_{fb}) which form a couple [$N_{fh}(c+f)$] and to moments (M_f) in each face (Fig. 1c). Again, forces developed in the relatively low-stiffness core are insignificant when compared to the forces in the faces.

Shearing deformation in a layered panel is due primarily to deformation of the relatively low-stiffness core material and can be a significant part of the total deformation of a layered structure. For a layered beam, transverse shear leads to the deformation shown in Fig. 1d. The presence of transverse shear deformation as a significant part of the deformation of a sandwich structure is a complicating factor when compared with single-layered structures in which shear deformation is often not significant. Likewise, the presence of significant shear deformation in layered cranial bone could complicate modeling and analysis of the brain case.

Diploë core compression in the region of loading is usually not a major deformation mechanism for layered structure as a whole, but it can lead to penetration of the structure. This form of deformation and failure has been related to skull damage by Melvin and Fuller (1970) and Hodgson *et al.* (1970).

Membrane deformation of the skull, diploë compression, and skull punch-through have been previously studied and were not pursued in this study. Bending and shearing deformations of layered cranial bone have not been previously studied, are significant to skull deflection under radial loading, and are the primary subject of the present study.

The resistance or stiffness of sandwich structures to bending and shearing deformations may be determined experimentally from flexure in three-point bending of beam samples taken from the sandwich structure (Kelsey *et al.* 1958). The mid-span deflection of a simply supported beam in symmetrical three-point bending is given in equation 1.

$$\frac{\delta}{P}=\frac{1}{48EI}L^3+\frac{1}{4GA}L+H, \qquad (1)$$

where: δ = mid-span deflection
P = mid-span load
L = span length
EI = bending stiffness
GA = shearing stiffness
H = non-span related compliance.

Deflection due to bending is related to the span length to the third power, and the deflection due to shear to the span length to the first power. Beam testing at a number of different span lengths allows the bending and shear deflections to be separated. Mid-span deflection (δ) is divided by mid-span load (P) to form a convenient parameter commonly

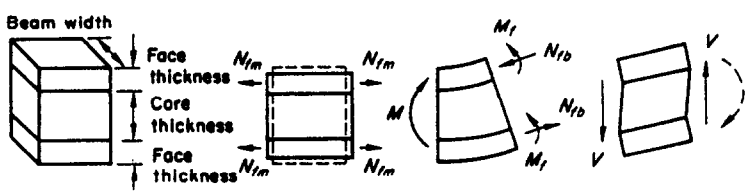

Fig. 1. Layered beam element and deformations; a. layered beam element; b. membrane deformation; c. bending deformation; d. shearing deformation.

called compliance (δ/P) which is the deflection of a member for a unit load. For use of equation 1, it is assumed that the beam is straight, its mechanical properties and structural geometry are invariant along its span, and its load-deflection response is linear. If samples cut from cranial bone can be found which may be considered straight and uniform, then the three-point bending technique may be applied for the determination of the bending and shearing stiffness of layered cranial bone.

Sandwich structure technology includes a theory which relates the structural geometry and constituent material properties of layered beams to their flexural response. This theory was developed by van der Naut, and is presented in a book by Plantema (1965). It considers deflection in a cantilevered sandwich beam due to bending, extension, and shear in the individual faces, and shear in the core. The equations for the mid-span compliance are written here for the similar three-point bending case.

$$\frac{\delta}{P} = \frac{\delta_{fb}}{P} + \frac{\delta_{cs}}{P} + \frac{\delta_{fs}}{P} \qquad \text{total mid-span compliance} \qquad (2)$$

where:

$$\frac{\delta_{fb}}{P} = \frac{1}{48}\frac{L^3}{(EI)_1} - 2\frac{(EI)_f \delta_{cs}}{(EI)_1 P} \qquad \text{bending compliance}$$

$$\frac{\delta_{cs}}{P} = \frac{L}{4S}\left[1 - \frac{2\tanh(\alpha L/2)}{\alpha L}\right] \qquad \text{compliance due to core shear}$$

$$\frac{\delta_{fs}}{P} = \frac{\tanh(L\alpha/2)}{2\alpha(S+2S_f)} \qquad \text{compliance due to face shear}$$

$$\alpha = \left[\frac{S(S_f)}{(S+2S_f)(EI)_f}\right]^{1/2} \qquad \text{stiffness ratio}$$

$$S_f = G_f f w \qquad \text{face shear stiffness}$$

$$S = \frac{(c+f)^2}{c} G_c w \qquad \text{core shear stiffness}$$

$$(EI)_f = \frac{1}{12} f^3 E_f w \qquad \text{individual face bending stiffness}$$

$$(EI)_1 = \frac{1}{2} f (c+f)^2 E_f w \qquad \text{bending stiffness due to face normal forces}$$

$$(EI)_b = (EI)_1 + 2(EI)_f \qquad \text{total bending stiffness}$$

$$G_f = \frac{E_f}{2(1+\nu_f)} \qquad \text{face shear modulus}$$

$\nu_f = 0{\cdot}3$ Poisson's ratio assumed for faces
E_f elastic modulus of faces
G_c core shear modulus
f face thickness
c core thickness
w beam width
L span length.

Under severe trauma the skull often fails due to initiation and propagation of linear fractures. The length of the linear fractures are usually much larger than the dimensions of the beam samples in this study. Therefore linear fracture propagation was not studied here. However, fracture initiation is a local occurrence of material rupture, and beam testing can be used to induce fracture of cranial bone samples. With appropriate theory the beam loading can be related to the induced strain field which leads to material rupture and beam failure.

In a layered beam normal strains (tensile and compressive) in the beam faces accompany bending deflection (Fig. 1c) and are essentially unaffected by shearing deflection (Fig. 1d). The strains in the faces can be related to the moment carried by the section using the strength-of-materials approach:

$$\epsilon = \frac{M(f + c/2)}{(EI)_b}. \qquad (3)$$

where ϵ is the surface strain, M is the moment carried by the section, $(f + c/2)$ is the beam half-thickness, and $(EI)_b$ is the total beam bending stiffness from equation 2. This moment–strain relationship incorporates section geometry and material properties, and is a theoretical basis for relating the failure behavior of compact cranial bone to the failure of the layered cranial bone structure. With the application of strain gages to the outer surfaces of beam samples this moment–strain relationship can be experimentally investigated.

EXPERIMENTAL TECHNIQUE

Eight beam samples were cut from the layered parietal bone of four embalmed calvaria. The axes of the samples were generally parallel to and from 1–2½ in. to either side of the sagittal suture. The samples were milled to tested shape with a Unimat-SL and stored at room temperature in closed glass bottles with damp gauze sponges to maintain sample moisture. All cutting was done on surfaces perpendicular to the bone tables, and care was exercised not to modify the inner and outer surfaces more than necessary for seating of test load application points. A typical layered cranial bone beam is shown in Fig. 2.

Symmetrical three-point bending tests were performed with an Instron testing machine and the bending apparatus shown in Fig. 3. The bending fixture was very stiff relative to the beam sample so that the deflection of the beam could be monitored using a linear variable differential transformer (LVDT) mounted as shown in Fig. 3. The applied load was monitored using an Instron 1,000 lb tension–compression load cell, and displayed on a trace storing oscilloscope against the mid-span deflection as monitored by the LVDT. Bending tests were conducted for each beam at quasi-static deformation rates and at spans ranging from 0·750–1·875 in. in 0·125 in. steps. Beams were supported on the inner table and loaded at mid-span on the outer table ('normal' orientation, *N*) and inverted and loaded at mid-span on the inner table ('inverted' orientation, *I*). Because modification of the table surfaces was avoided as much as possible, particular orientations and spans for some of the beams were not tested due to poor loading surface contact conditions. Beams were initially loaded, partially unloaded, and then reloaded repeatedly.

For the application of layered beam theory (equation 2), the cranial bone beams were considered to be three-layered structures. The layers were differentiated subjectively and the layer thicknesses were measured with a dial micrometer under a 10× microscope (Table 1). Beam widths, layer thicknesses, and total thicknesses were measured at seven sites spaced 0·25 in. apart along the beam axis on both machined surfaces. The middle measurement site coincided with the mid-span of the test section. The first number of the sample designation indicates the beam

Table 1. Layered beam geometry

Beam number	Weighted mean layer thickness (in.) Inner table	Diploë	Outer table	Total	Width (in.)
1–1	0·061	0·127	0·057	0·246	0·375
2–1	0·061	0·124	0·068	0·252	0·353
3–1	0·046	0·168	0·051	0·268	0·357
1–2A	0·051	0·096	0·066	0·213	0·423
1–2 B	0·059	0·088	0·068	0·215	0·277
2–2	0·046	0·149	0·066	0·261	0·365
1–5 A	0·050	0·161	0·070	0·281	0·728
1–5 B	0·051	0·166	0·065	0·282	0·501
2–5 A	0·053	0·177	0·065	0·295	0·582
2–5 B	0·050	0·181	0·069	0·299	0·376
1–6 A	0·068	0·088	0·079	0·235	0·468
1–6 B	0·068	0·095	0·074	0·236	0·331

number from a particular calvarium and the second number indicates the calvarium. The tested beam sections had a radius of curvature of at least ten beam thicknesses so that this curvature was not considered significant for the samples and tests of the present study (Seely and Smith, 1965). The letters (A) and (B) indicate samples that were tested, then milled, and re-tested to determine sample width effects.

To study failure of layered cranial bone, strain gages were bonded to the inner and outer mid-region surfaces of layered beams. These beams had been used in the study of the reversible response of layered cranial bone. Strain gages allowed the verification of the moment–strain relationship (equation 3) and the monitoring of beam surface strains as the beams were loaded to failure.

Beam number 1–6 was loaded in symmetrical three-point bending with a total span length of 1·250 in. The remaining beams were loaded in symmetrical four-point bending with a major span of 2 in. and a minor span of 1 in. In the four-point bending tests, loading was applied to the samples through a block which was free to rotate, insuring that the mid-region was pure bending. Beams were loaded and then unloaded while the strain in the gage in compression and the load were monitored against bending fixture displacement as sensed by the LVDT. They were then loaded to failure with the tensile strain gage and load monitored against fixture displacement.

The reversible load–deflection response of a layered beam is primarily a function of the properties of beam constituent materials and the structural geometry of the entire tested beam section. The failure response of the same beam is primarily a function of the factors which affect the local material rupture leading to fracture of the beam sample. These factors are the local structural geometry and material properties of the ruptured region, and they are the primary determinants of the strain field which must be supported by a beam sample under load. For beam samples 2–1, 3–1, and 2–5 the layer thicknesses in the mid-regions to which strain gages were attached were significantly different from those given in Table 1. These mid-region thicknesses are given in Table 2 and have been used for these beams in the application of equation 3. For the remaining beams, the average thicknesses given in Table 1 were sufficiently close to the mid-region dimensions to be used in the moment–strain predictions.

RESULTS AND DISCUSSION

Introduction

Although an effort was made to include beam samples with material properties and geometric characteristics which represent the range of human population, beam samples were selected from the available calvaria with primary attention given to geometric requirements necessary for analytic interpretation of the test data. The results are indicative of the flexural response of cranial bone and support

Table 2. Layered beam mid-span geometry

Beam	Mid-span layer thickness Inner table	Diploë	Outer table	Total
2–1	0·041	0·133	0·059	0·234
3–1	0·038	0·169	0·051	0·258
2–5	0·042	0·191	0·064	0·297

the appropriate application of layered structure technology to the study of this response. However, use of numerical values presented in head modeling should be made with an appreciation for the limited data from which they were determined. For the purpose of data presentation and analysis, beam width has been incorporated with compliance into a compliance parameter, $\delta w/P$, which facilitates study of width dependence of flexural properties of cranial bone and the comparison of the response of beams of different widths.

Reversible layered beam test results

For eight beams cut from the layered regions of four embalmed calvaria, the resistance to bending and shearing deformation has been determined by multi-span three-point flexure tests. The basis of this determination is compliance parameter data plotted against test span length, Figs. 4–11. Note in Figs. 7, 9, and 11 that reducing the beam width had no significant effect on the flexural response of the respective samples. In contrast, reducing the beam width of beam sample 2–5 (Fig. 10) significantly reduced its compliance. This inconsistency with other results could be due to poor loading of sample 2–5A, leading to significant non-span related deflection which was not present in sample 2–5B. Beam samples 2–2, 1–5B, and 1–6B were tested

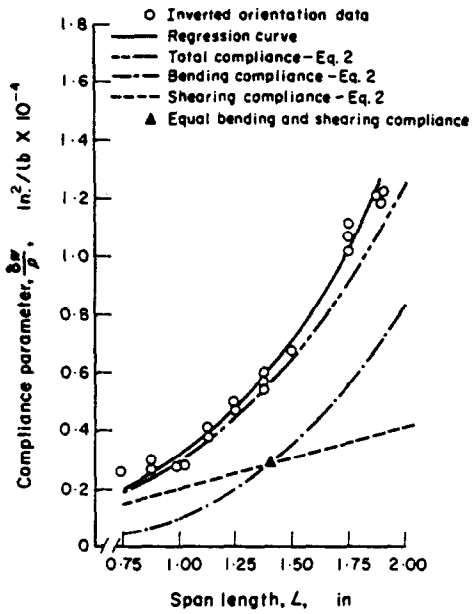

Fig. 5. Compliance parameter vs. span-beam sample 2–1.

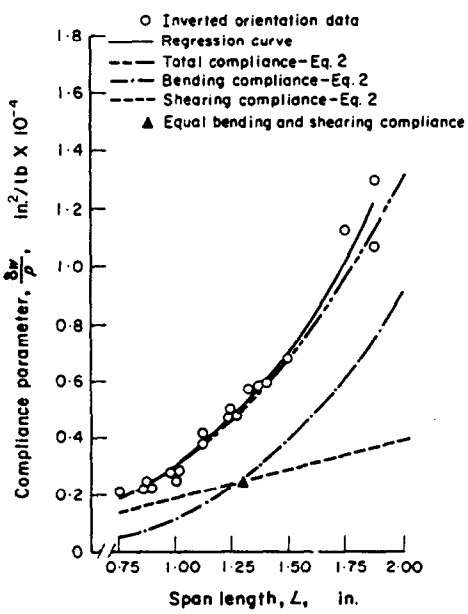

Fig. 4. Compliance parameter vs. span-beam sample 1–1.

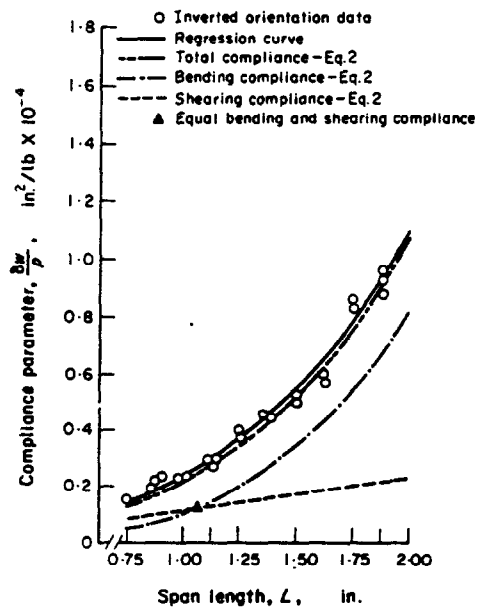

Fig. 6. Compliance parameter vs. span-beam sample 3–1.

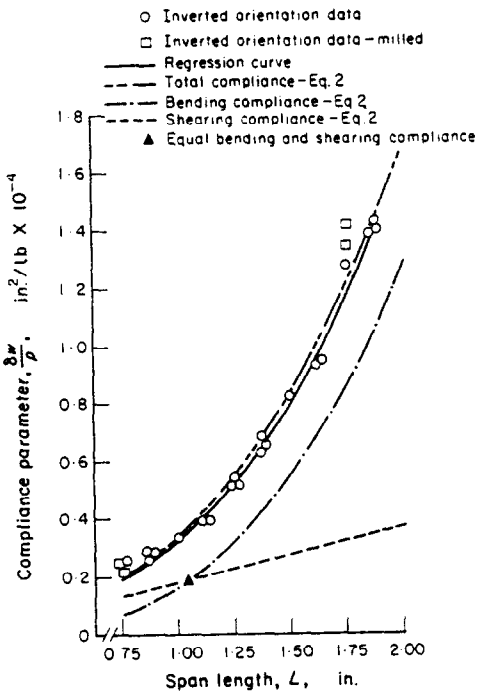

Fig. 7. Compliance parameter vs. span-beam sample 1–2.

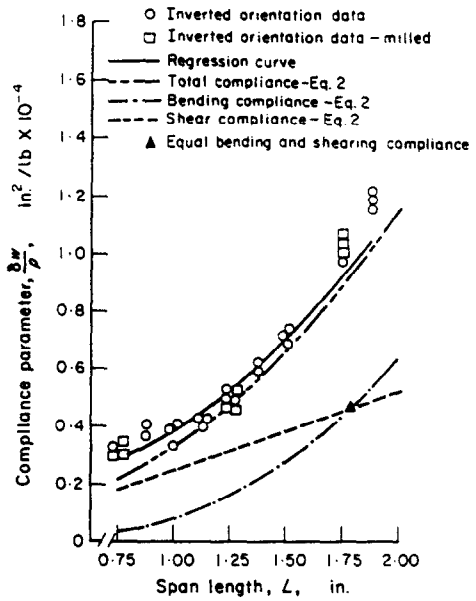

Fig. 9. Compliance parameter vs. span-beam sample 1–5.

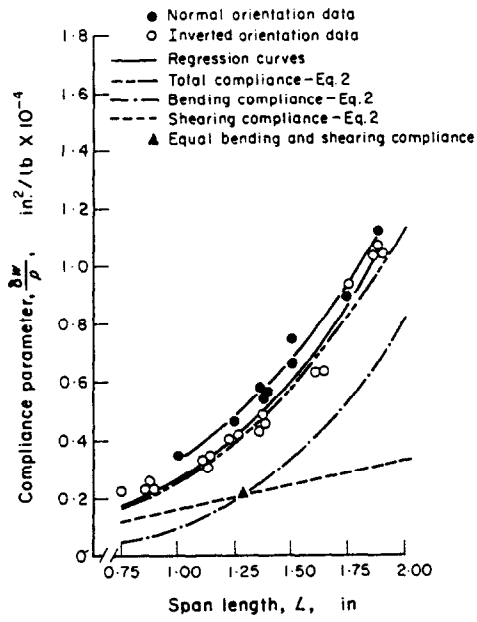

Fig. 8. Compliance parameter vs. span-beam sample 2–2.

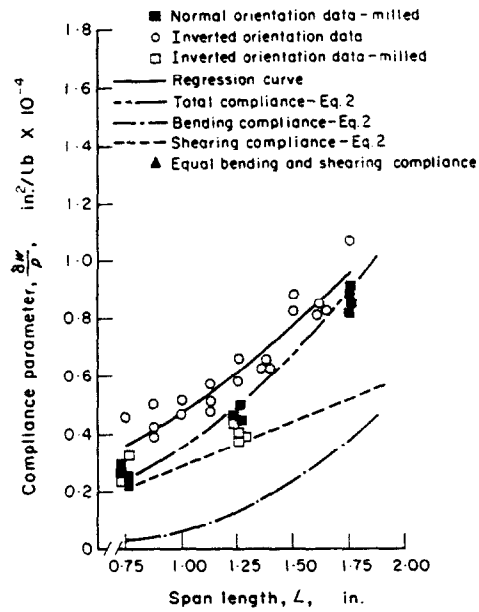

Fig. 10. Compliance parameter vs. span-beam sample 2–5.

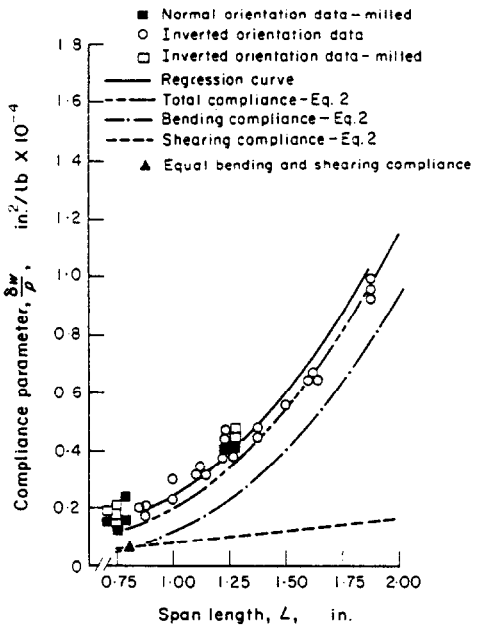

Fig. 11. Compliance parameter vs. span-beam sample 1–6.

in both the normal and inverted orientations (Figs. 8, 9, and 11 respectively). Sample 2–2 was slightly stiffer throughout the tested span range in the inverted orientation than in the normal orientation. Because of a constant offset, this orientation effect appears to be due to a non-span related effect. There was no orientation effect in the response of samples 1–5B and 1–6B.

Multiple linear regression was used to fit a polynomial with third- and first-order terms in span length to the compliance parameter vs. span length data. The regression curves are shown in Figs. 4–11. By equation 1, the bending stiffness, $\overline{EI}$, and shearing stiffness, $\overline{GA}$, for each beam can be calculated based on regression coefficients of the third and first order, respectively. The stiffness $\overline{EI}$ and $\overline{GA}$ are presented in Table 3 paired with quantities $\Delta\overline{EI}$ and $\Delta\overline{GA}$ which were calculated from the standard errors of the regression coefficients upon which the stiffnesses are based. These quantities reflect how well the stiffnesses are determined by regression analysis of the compliance data.

A modulus of elasticity, $\bar{E}$, can be determined by dividing the bending stiffness of a beam by the second moment of its cross-sectional area, including the area of the porous

Table 3. Flexure characteristics of layered cranial bone

Beam number and orientation		1–1*I*	2–1*I*	3–1*I*	1–2*I*	2–2*N*	2–2*I*	1–5*I*	2–5*N*	1–6*I*
Bending stiffness from beam tests (1 bf-in.²)	$\overline{EI}$	564	534	706	513	710	622	2100	2770	747
	$\Delta\overline{EI}$	50	32	58	27	67	57	260	1340	88
Bending stiffness from beam theory (1 bf-in.²)	$(EI)_b$	680	713	718	541	756	756	1878	1705	819
Equivalent elastic modulus from beam tests (1 bf/in.² × 10⁶)	$\bar{E}$	1·21	1·13	1·23	1·48	1·31	1·15	1·54	2·22	1·38
	$\Delta\bar{E}$	0·11	0·07	0·10	0·08	0·12	0·11	0·19	1·07	0·16
Equivalent elastic modulus from beam theory (1 bf/in.² × 10⁶)	*EBAR*	1·48	1·51	1·26	1·59	1·39	1·39	1·38	1·34	1·62
Shear stiffness from beam tests (lb × 10⁶)	$\overline{GA}$	5·72	5·48	8·08	7·60	4·20	9·52	6·19	3·71	12·1
	$\Delta\overline{GA}$	1·93	1·54	3·00	2·27	0·80	5·35	0·88	0·77	8·2
Equivelent shear modulus from beam tests (1 bf/in.² × 10³)	$\bar{G}$	61·9	65·7	84·4	83·9	44·1	99·9	30·1	21·6	108
	$\Delta\bar{G}$	20·9	17·4	31·3	25·1	8·4	56·2	4·3	4·5	73
Core shear modulus from beam tests (1 bf/in.² × 10³)	$\bar{G}_c$	42·0	43·0	77·5	79·7	32·1	72·7	22·1	16·2	60·2
	$\Delta\bar{G}_c$	14·2	11·4	28·5	23·9	6·1	41·1	3·2	3·4	4·1
Core shear modulus (1 bf/in.² × 10³)	G_c	45	40	75	50	50	50	30	20	100

layer. This modulus is a property of a homogeneous material which could be used in a structure of the same exterior geometry as layered cranial bone to exhibit the same bending response as layered cranial bone. Similarly, dividing the shear stiffness of a bone by its cross-sectional area yields an equivalent homogeneous material shear modulus, $\bar{G}$. If the shear deflection of the beam is attributed entirely to shear deformation in the porous core, then the shear modulus of the core material, $\bar{G}_c$, also may be calculated (Plantema, 1965). The moduli $\bar{E}$ based on the bending stiffnesses $\overline{EI}$, and $\bar{G}$ and $\bar{G}_c$ based on $\overline{GA}$ are presented in Table 3 with the quantities $\Delta\bar{E}$, $\Delta\bar{G}$, and $\Delta\bar{G}_c$.

These stiffnesses are all well determined by regression analysis of the experimental data. The variations based on one standard deviation is generally less than 10 per cent. Notable exceptions are the bending stiffnesses as determined by the first and third order/regressions for beam samples 1–5 and 2–5. Because the variation in the bending stiffnesses is also reflected in the variations of the moduli calculated from them, the effective elastic moduli are also well determined by the regression analysis.

Layered beam theory results

Layered beam theory relates the component material properties and structural geometry of layered beams to their response to transverse loading. The geometric information needed for the application of layered beam theories to the study of the tested beams has been presented in Tables 1 and 2. Appropriate constituent material properties remain to be specified. The results of tension tests conducted on samples taken from the embalmed calvaria from which the layered beam samples taken agree with results for unembalmed compact cranial bone at the same strain rate (Wood, 1969). Because the compact bone tables in the layered beam tests were strained at a rate of approximately 0·01 in./in.sec, Wood's mean value of elastic modulus, $1{\cdot}72 \times 10^6$ psi, for that rate was used in the theoretical calculations for this study. The shear moduli of the diploë for the various layered beam samples were taken as half the respective compressive elastic moduli. This shear moduli determination was based on the assumption that the elastic moduli. This shear moduli determination was based on the assumption that the Poisson's ratio for an open cell material is zero (Hoff–Mautner, 1948). These moduli, are given in the bottom row of Table 3.

The results of layered beam theory calculations are shown in Figs. 4–11. In all cases, the responses as determined by equation 2 closely agree with the responses measured in beam testing. The point at which bending and shearing compliance are equal is indicated for each theory by a triangle. Note that for most of the samples, the shear compliance was small compared to the bending compliance within the tested span range, and they were equal only at the shorter spans. Notable exceptions are samples 1–5 and 2–5 which have relatively thick, low modulus diploë. For these samples the shear compliance was a major factor in the

Table 4. Layered beam failure response

Beam number and orientation		2–1*I*	3–1*I*	2–2*N*	1–5*N*	2–5*N*	1–6*N*
Experimental	Inner gage	2·28	2·35	2·01	1·35	1·81	1·98
Strain/moment	Outer gage	2·92	2·73	1·42	1·16	1·72	—
(1/in.lb) × 10^{-4}	Average	2·60	2·54	1·70	1·26	1·77	1·98
Theoretical strain/moment (1/in.lb) × 10^{-4}		2·44	2·14	1·73	1·26	1·79	2·04
Strain at	Bending	—	0·76	0·46	0·38	0·33	0·62
failure (%)	Tension	—	0·77	0·43	0·50	0·50	0·41
Maximum moment (in.lb)		—	30·3	24·3	29·3	18·0	30·0
Max. moment/beam width (lb)		—	85·7	68·1	67·4	48·0	90·6

total deflection within the tested span lengths. The significance of shear deflection in layered cranial bone to the mechanics of head injury cannot be fully evaluated from these tests and analyses. Only through application of plate or shell theory and testing of larger samples which more closely describe the intact human skull can the importance of shear deflection be better determined.

To aid the study and comparison of theoretical and experimental results, the quantities $(EI)_b$ and $EBAR$ are given in Table 3 for each beam sample. The total bending stiffness, $(EI)_b$ of equation 2 is the mechanical parallel sum of the face membrane stiffness and the individual face bending stiffness. In a manner similar to the determination of $\bar{E}$, $EBAR$ is calculated by dividing $(EI)_b$ by the total beam cross-sectional area. Like the experimentally determined equivalent moduli, $EBAR$ is the theoretical modulus of elasticity of a material which could be used in the same geometry as the layered skull bone to have the same bending response as layered skull bone.

For the beams which were tested, milled, and re-tested (beam samples 1–2, 1–5, 2–5, and 1–6), the determinations of experimental and theoretical stiffnesses were based on the beam geometry as initially tested. Beam stiffnesses were not normalized with respect to beam width, and therefore are not directly comparable between samples. In contrast, the experimentally determined and theoretically calculated moduli do not reflect beam sample width and are comparable between samples.

The theoretically calculated total bending stiffnesses, $(EI)_b$, are generally higher than the comparable experimentally determined bending stiffnesses, $\bar{E}\bar{I}$, with the exceptions of samples 1–5 and 2–5. Considering the deviations in the experimentally determined stiffnesses, $\Delta\bar{E}\bar{I}$, these results support the use of equation 2 to compute the bending stiffness of layered cranial bone. Because the moduli, $\bar{E}$ and $EBAR$, are calculated in the same manner from the experimentally determined and theoretically calculated stiffnesses, the agreement which is present between the experimental and theoretical bending stiffnesses is also present between the effective elastic moduli. The effective moduli, $\bar{E}$ and $EBAR$, are somewhat lower than the modulus of the compact table material, $1{\cdot}72 \times 10^6$ psi, as would be expected.

From the first order term of the first and third order regression, the shearing stiffnesses of the beams tested were calculated. The values of these stiffnesses, $\overline{GA}$, are less well determined than the bending stiffnesses. From these experimentally based values of shear stiffness, effective shear moduli have been calculated, $\bar{G}$ (Table 3). With the assumption that the shear deflection of the beam samples is mainly due to shear deformation of the diploë core, the shear moduli of the diploë in the tested beam samples, $\bar{G}_c$, has been determined (Table 3). In general, the values of core shear modulus, G_c, used for theoretical calculation were within the first standard deviation range of the beam-based values, $\bar{G}_c$. Considering the accuracy with which the shear properties of porous materials can be determined by beam testing or compression testing, the results support the use of the layered beam theories for the incorporation of diploë core properties into the theoretical calculation of the mechanical response of layered cranial bone.

Failure of layered beams

With strain gages bonded to their inner and outer table surfaces, the layered cranial bone beam samples used in the study of reversible response were repeatedly loaded, and then loaded to failure to study their failure response. When loaded and unloaded, the strain on the side of the beam in compression was monitored. All beams, except beam samples 2–1 and 3–1, were loaded so that the inner table was in tension. Beam samples 2–1 and 3–1, were loaded so that the inner tables were placed in compression. Beams 1–1 and 1–2 were not used in this part of the study.

Because the strain and load were both

monitored against bending fixture deflection rather than against each other, cross-plotting was necessary to form a strain–moment plot. Figure 12 is typical of the strain–moment plots. The slope of the initial linear region was taken as the experimentally determined strain–

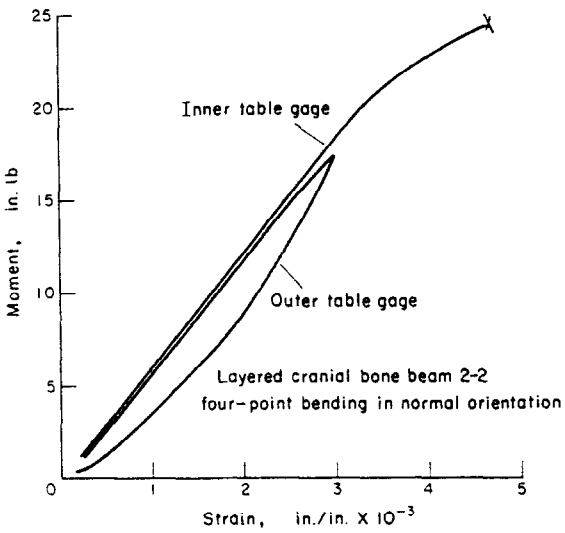

Fig. 12. Typical moment–strain cross-plot.

moment relation for each test. These ratios are given in Table 4. The values given for each gage location are in most cases the average of a few replications. Because the beams were not necessarily symmetrical with respect to the plane of zero deformation and the strain gages were bonded to bone surfaces which were not perfectly smooth, the strain–moment ratios determined by the inner and outer table gages for the same beam were not equal. The average of these ratios closely agrees with the ratios calculated using equation 4. This agreement supports the use of the strength of materials approach, as expressed in equation 4, for the relationship of the moment supported by a layered cranial bone beam and the associated surface strains.

The beams were loaded in four-point bending until they failed. The failure initiated as a crack on the tensile side of the beam which propagated through the table under tension, through the diploë, and through the other bone table. The fracture surfaces were consistently perpendicular to the beam axes, and the surface appearance was similar to the fracture surfaces of cranial bone samples loaded to failure in tension. Unfortunately the fracture occurred outside the gaged regions so that the gages did not monitor the strain levels which were directly associated with failure, but rather the strain levels which were imposed on the gaged region when failure occurred elsewhere. The strain at failure was monitored in the tensile gage and has been given in Table 4. Also given are the failure strains for tensile samples taken from the same calvaria as the beam samples. Considering the variability of material properties (Wood, 1969), these strain values generally agree. However, the strain levels at failure in the beams were slightly lower than the average failure strain for cranial bone tested in tension at comparable strain rates (Wood, 1969). The maximum moments which the beams supported are also given in Table 4. Calculation of a stress at failure from maximum moment data would be questionable considering the assumptions necessary for equation 4, and the non-linear behavior of cranial bone near failure.

SUMMARY AND CONCLUSIONS

As an essential step in the understanding of the human skull as a structure and of the mechanics of head injury, layered cranial bone samples were mechanically tested and analytically studied. Beams taken from the layered regions of embalmed calvaria were repeatedly tested in three-point bending at various span lengths to determine the resistance of layered cranial bone to bending and shearing deflection. These beams were also strain gaged and loaded to failure in four-point bending to study the failure of layered cranial bone. Layered beam theory was applied to the study of layered cranial bone, and was found to provide a valid relationship between the constituent material properties and structural geometry of layered cranial

bone, and its response as a layered structure. Specific conclusions are listed below.

Results of repeated testing in three-point bending at various spans of beams cut from the layered regions of embalmed calvaria indicate that:

(1) there is no significant effect of beam width on the reversible flexural response of layered cranial bone, and

(2) there is no significant effect of beam test orientation, normal or inverted, on the reversible flexural response of layered cranial bone.

Multiple linear regression analysis of results from three-point bending tests of layered cranial bone beams leads to:

(1) separation of the effects of bending and shearing deformation on the total beam deflection, leading to determination of the stiffnesses to bending and shearing deflection of layered cranial bone;

(2) an indication of the accuracy with which these bending and shearing stiffnesses are experimentally determined, and

(3) determination of elastic and shear moduli of hypothetical homogeneous materials which may be used in structures of the same total thickness as layered cranial bone to respond in bending and shear in the same manner as the layered structure.

The appropriate application of layered beam theories to the study of the reversible response of layered cranial bone provides:

(1) theoretical, calculated, flexural response which generally agrees with experimentally measured response throughout the tested beam span range;

(2) a basis for calculating the separate effects and relative magnitude of bending and shearing deflection of layered cranial bone, and

(3) a valid relationship between the constituent material properties and structural geometry and the flexural response of layered cranial bone.

Four-point bending to failure of layered cranial bone beams with strain gages attached to their surfaces:

(1) verified the use of equation 4 for the determination of surface strain levels induced in layered cranial bone beams loaded by moments;

(2) produced levels of surface strain at failure in bending which are generally equal to failure strain levels for compact cranial bone loaded in tension, and

(3) produced failure of layered cranial bone beams by crack initiation in a tensile strain field and propagation through the beam perpendicular to the beam axis.

REFERENCES

Hodgson, V. R., Brinn, J., Thomas, L. M. and Greenberg, S. W. (1970) Fracture behavior of the skull frontal bone against cylindrical surfaces. *Proc. 14th Stapp Car Crash Conf.*, Ann Arbor, Michigan.

Hoff, N. J. and Mautner, S. E. (1948) Bending and buckling of sandwich beams. *J. Aeronaut. Sci.* **15**, 707–720.

Kelsey, S., Gellatly, R. A. and Clark, B. W. (1958) The shear modulus of foil honeycomb cores. *Aircr. Engng* **30**, 294–302.

Melvin, J. W. and Fuller, P. M. (1970) Effect of localized impact on the human skull and patella. *Proc., 14th Annual Conf. of Am. Assoc. for Automobile Med.*

Melvin, J. W., Robbins, D. H. and Roberts, V. L. (1969) The mechanical behavior of the diploë layer of the human skull in compression. Developments in Mechanics, *Proc., 11th Midwest Mech. Conf.* **5**, 811–818.

Plantema, F. J. (1965) *Sandwich Construction, The Bending and Buckling of Sandwich Beams, Plates, and Shells*. Wiley, New York.

Seely, F. B. and Smith, J. O. (1965) *Advanced Mechanics of Materials*. 2nd edn, pp. 148–153. Wiley, New York.

Wood, J. L. (1969) Mechanical properties of human cranial bone in tension. Doctoral dissertation, The University of Michigan. Also presented as; Tensile properties of bone at high strain rates, at 1970 ASME Winter Annual Meeting, Paper No. 70-WA/BHF-10.

NOMENCLATURE

w	beam width (in.)
f	face thickness (in.)
c	core thickness (in.)
L	span length (in.)
N_{fm}	force in face due to membrane deformation (1 bf)
N_{fb}	force in face due to bending deformation (1 bf)
M	moment applied to beam element (1 bf-in.)
M_f	moment in face due to bending deformation (1 bf-in.)
V	shear force applied to beam element (1 bf)
P	mid-span load (1 bf)
δ	mid-span deflection (in.)
$\frac{\delta}{P}$	compliance (in./1 bf)
$\frac{\delta w}{P}$	compliance parameter (in².1 bf)

$\frac{\delta_{fb}}{P}$ bending compliance (in./1 bf)

$\frac{\delta_{fs}}{P}$ compliance due to face shear (in./1 bf)

$\frac{\delta_{cs}}{P}$ compliance due to core shear (in./1 bf)

EI bending stiffness (1 bf-in^2.)

$(EI)_f$ individual face bending stiffness (1 bf-in^2.)

$(EI)_1$ bending stiffness due to face normal forces (1 bf-in^2.)

$(EI)_b$ total bending stiffness (1 bf-in^2.)

$\overline{EI}$ bending stiffness from beam tests (1 bf-in^2.)

E_f elastic modulus of faces (1 bf/in^2.)

$\bar{E}$ equivalent elastic modulus from beam tests (lb/in^2.)

$EBAR$ equivalent elastic modulus from beam theory (1 bf/in^2.)

S_f face shear stiffness (1 bf)

S core shear stiffness (1 bf)

GA shear stiffness (1 bf)

$\overline{GA}$ shear stiffness from beam tests (1 bf)

G_f face shear modulus (1 bf/in^2.)

G_c core shear modulus (1 bf/in^2.)

$\bar{G}$ equivalent shear modulus from beam tests (1 bf/in^2.)

$\bar{G}_c$ core shear modulus from beam tests (1 bf/in^2.)

ν_f Poisson's ratio assumed for faces

α stiffness ratio

H non-span related compliance (in./1 bf)

ϵ surface strain (in./in.)